microbial cell

Research Article

www.microbialcell.com

Arsenite treatment induces Hsp90 aggregates distinct from conventional stress granules in fission yeast

Naofumi Tomimoto[a], Teruaki Takasaki[a] and Reiko Sugiura*

Laboratory of Molecular Pharmacogenomics, Department of Pharmaceutical Sciences, Faculty of Pharmacy, Kindai University, Higashiosaka, Osaka 577-8502, Japan

*Corresponding Author:
Reiko Sugiura, TEL: +81-6-4307-3642; FAX: +81-6-6730-1394; E-mail: sugiurar@phar.kindai.ac.jp

[a]Equal contribution as a first author.

ABSTRACT Various stress conditions, such as heat stress (HS) and oxidative stress, can cause biomolecular condensates represented by stress granules (SGs) via liquid-liquid phase separation. We have previously shown that Hsp90 forms aggregates in response to HS and that Hsp90 aggregates transiently co-localize with SGs as visualized by Pabp. Here, we showed that arsenite, one of the well-described SG-inducing stimuli, induces Hsp90 aggregates distinct from conventional SGs in fission yeast. Arsenite induced Hsp90 granules in a dose-dependent manner, and these granules were significantly diminished by the co-treatment with a ROS scavenger N-acetyl cysteine (NAC), indicating that ROS are required for the formation of Hsp90 granules upon arsenite stress. Notably, Hsp90 granules induced by arsenite do not overlap with conventional SGs as represented by eIF4G or Pabp, while HS-induced Hsp90 granules co-localize with SGs. Nrd1, an RNA-binding protein known as a HS-induced SG component, was recruited into Hsp90 aggregates but not to the conventional SGs upon arsenite stress. The non-phosphorylatable eIF2α mutants significantly delayed the Hsp90 granule formation upon arsenite treatment. Importantly, inhibition of Hsp90 by geldanamycin impaired the Hsp90 granule formation and reduced the arsenite tolerance. Collectively, arsenite stimulates two types of distinct aggregates, namely conventional SGs and a novel type of aggregates containing Hsp90 and Nrd1, wherein Hsp90 plays a role as a center for aggregation, and stress-specific compartmentalization of biomolecular condensates.

doi: 10.15698/mic2024.07.829
Received originally: 08. 12. 2023;
in revised form: 14. 06. 2024,
Accepted: 18. 06. 2024
Published: 19. 07. 2024

Keywords: Hsp90, Aggregates, Stress granules, Fission yeast, Arsenite

Abbreviations:
CHX - cycloheximide,
GA - geldanamycin,
HS - heat stress,
PACs - protein aggregate centers,
NAC - N-acetylcysteine,
ROS - reactive oxygen species,
SGs - stress granules.

INTRODUCTION

Stress granules (SGs) are dynamic cytoplasmic non-membranous condensates that can rapidly assemble and disassemble in response to environmental stimuli, including heat, hypoxia, oxidative stress, arsenite, and nutrient deprivation [1–7]. SGs are composed of 40S ribosomal subunits, translation initiation factors, poly(A)+ mRNAs, and various RNA-binding proteins (RBPs), as represented by G3BP [2, 6, 8]. Besides their role in promoting cell survival by condensing translationally stalled mRNAs, SGs constitute signaling hubs and influence multiple signaling pathways by sequestering and intercepting various signaling components represented by mTOR and PKC/MAPK signaling [9–12].

Recent advances in SG biology highlighted the heterogeneity of SGs in their RNA and protein content leading to the idea that various SG subtypes exist. For example, proximity labeling proteomic analyses uncovered cell-type- and stress-specific SG composition [13, 14], thus expanding our knowledge of the composition of various SGs. However, the regulatory mechanisms of how each component of SGs is recruited into specific granules remain poorly understood.

Hsp90 is a highly conserved chaperone protein involved in various cellular processes such as signal transduction and stress response [15–17]. We have previously characterized the spatiotemporal distribution of Hsp90 in fission yeast in response to heat stress (HS) and demonstrated that Hsp90 is transiently incorporated into SGs as evidenced by the co-localization with Pabp upon high-HS at 45°C, whereas Hsp90 forms aggregates under mild HS (at 37°C), a condition where no SGs are formed [18]. Thus, Hsp90 forms distinct aggregates in response to the same stress (HS) at different intensities. Here, we demonstrated that Hsp90 forms a novel type of

aggregates in response to arsenite treatment, a well-described SG inducer. Unexpectedly, arsenite-induced Hsp90 aggregates do not overlap with conventional SGs as represented by eIF4G or Pabp, whereas HS-induced Hsp90 aggregates reside in SGs. Notably, an RNA-binding protein Nrd1, one of the components of HS-induced SGs [19], was targeted to Hsp90 aggregates induced by arsenite but not to conventional SGs. These data demonstrated the existence of a stress-specific mechanism that differentially compartmentalizes selective molecules to respective biological condensates. We also demonstrated the importance of Hsp90 activity in the formation of Hsp90 granules and tolerance to arsenite. Given the conserved role of Hsp90 as a molecular chaperone protein, our findings may suggest a novel type of arsenite-induced biological condensates, wherein Hsp90 plays a key role in maintaining its integrity.

RESULTS

Arsenite induces cytoplasmic Hsp90 granule formation

In fission yeast, Hsp90 is present diffusively in the cytoplasm under non-stressed conditions (27°C) and our previous findings showed that severe HS (45°C) induces transient cytoplasmic Hsp90 granules which overlap with stress granules (SGs) [18]. On the other hand, under moderate HS conditions (37°C), wherein SGs were not formed, Hsp90 formed persistent granules [18]. In the present work, we sought to investigate whether another SG-inducer arsenite alters the spatial distribution of Hsp90.

We first measured the temporal dynamics of Hsp90 distribution at multiple time points during the 120-minute arsenite treatment at various concentrations ranging from 0.2 to 1.0 mM. Induction of Hsp90 granules was observed in the cells treated with 1.0 mM arsenite for 30 min, which further increased upon 60 min treatment (**Figure 1A**). Quantification of the Hsp90 granule formation as evaluated by the percentage of the cells harboring the cytoplasmic Hsp90 granules (**Figure 1B**) and the number of Hsp90 granules per cell in Hsp90 granule-positive cells (**Figure 1C**) confirmed that arsenite-mediated induction of Hsp90 granules occurred within 30 min (when treated with 0.5 mM and 1.0 mM arsenite) peaking at 60 min and persisted for 120 min after treatment. Upon 0.2 mM arsenite treatment, the appearance of the Hsp90 granules was slower (after 60 min) and the induction of Hsp90 aggregates was less intense than at higher concentrations of arsenite treatment. Thus, higher concentrations of arsenite treatment induced faster and stronger induction of Hsp90 granule formation than lower concentrations of arsenite treatment, showing dose-dependent effects of arsenite on Hsp90 aggregation. Quantification of the size of Hsp90 aggregates also showed that higher concentrations of arsenite treatment induced larger Hsp90 granules more quickly than did lower concentrations of arsenite (**Figure 1D**). The number of Hsp90 granules per cell reached plateaus at around 30-60 min arsenite exposure and the size of Hsp90 granules became larger during incubation, suggesting the existence of the fusion mechanism of Hsp90 dots. It should be noted that even the lowest concentration of 0.2 mM arsenite with minimal impact on cell growth [20] can induce Hsp90 granule assembly.

Arsenite also stimulates nuclear localization of Hsp90 in a dose-dependent manner (**Figure 1A**, arrowheads). The nuclear fluorescence of Hsp90-GFP was observed in cells treated with 0.5 and 1.0 mM arsenite 60 min after treatment (**Figure 1A**). 0.2 mM arsenite did not induce Hsp90 nuclear translocation (**Figure 1E**). To validate the location of the nucleus, we co-expressed the nuclear envelope protein Cut11 tagged with mCherry with Hsp90-GFP. The fluorescence intensity plot of Hsp90-GFP and Cut11-mCherry with or without arsenite treatment confirmed that Hsp90 was concentrated in the nucleus upon arsenite treatment (**Figure 1F**). Thus, arsenite treatment stimulates cytoplasmic aggregation and nuclear enrichment of Hsp90 in a dose-dependent manner.

To characterize the nature of arsenite that induces Hsp90 granules, cells were co-treated with arsenite and a reactive oxygen species (ROS) scavenger n-acetylcysteine (NAC), and the results showed that arsenite-mediated Hsp90 granule formation was almost abolished by NAC (**Figure 1G**). Quantification of the number of Hsp90 granules confirmed the stimulatory effect of arsenite on the induction of Hsp90 granules and the impact of NAC to diminish arsenite-induced Hsp90 granules (**Figure 1H**). The nuclear enrichment of Hsp90 was also reduced by NAC (**Figure 1G**). Thus, oxidative stress is responsible for the spatial alteration of Hsp90 in response to arsenite treatment.

We also investigated the effects of other inducers of oxidative stress on Hsp90 granules and the results showed that $CuSO_4$ and $CdCl_2$, but not $ZnSO_4$, induced the aggregation of Hsp90 and co-treatment with NAC markedly reduced the aggregation of Hsp90 by $CuSO_4$ and $CdCl_2$ (Figure S1). Thus, some heavy metals, similar to arsenite, can induce the aggregation of Hsp90 via a ROS-involving mechanism.

Arsenite-induced Hsp90 granules do not overlap with conventional SGs

To further characterize the nature of arsenite-induced Hsp90 granules, we investigated whether Hsp90 resides in SGs upon arsenite treatment by visualizing endogenous eIF4G, a representative component of SGs, in cells expressing Hsp90-GFP. Upon 2.0 mM arsenite treatment for 180 min, eIF4G formed dot-like structures (**Figure 2A**, S2). Unexpectedly, none of the fluorescence of eIF4G dots overlapped with that of Hsp90 granules. Co-localization of Hsp90 and eIF4G was also analyzed by the intensity plot. The results showed that the fluorescence peaks of cytoplasmic Hsp90 granules (arrows) do not overlap with those of the eIF4G dots (arrowheads). Thus, arsenite induces two mutually exclusive biological condensates, namely, eIF4G dots and Hsp90 dots. We further analyzed whether or not Hsp90 dots co-localize with other components of representative SGs. These include Nxt3 (G3BP1 homolog), Pabp (Poly(A)-binding protein), eIF4E (eukaryotic translation initiation factor 4E), and the RNA helicase Ded1. Similarly to eIF4G, these representative components of conventional SGs formed dots upon 2.0 mM arsenite for 180 min (**Figure 2A**, S2). However, none of the components of canonical SGs co-localized with Hsp90 granules under arsenite treatment (**Figure 2A**), indicating that arsenite stimulates the induction of conventional SGs and Hsp90 granules and that these two biological condensates do not overlap.

We next analyzed whether the components of conventional SGs co-localize with Hsp90 upon HS as we have previously shown that Hsp90 transiently co-localizes with Pabp upon HS at 45°C. As shown in **Figure 2B**, all the components of SGs and

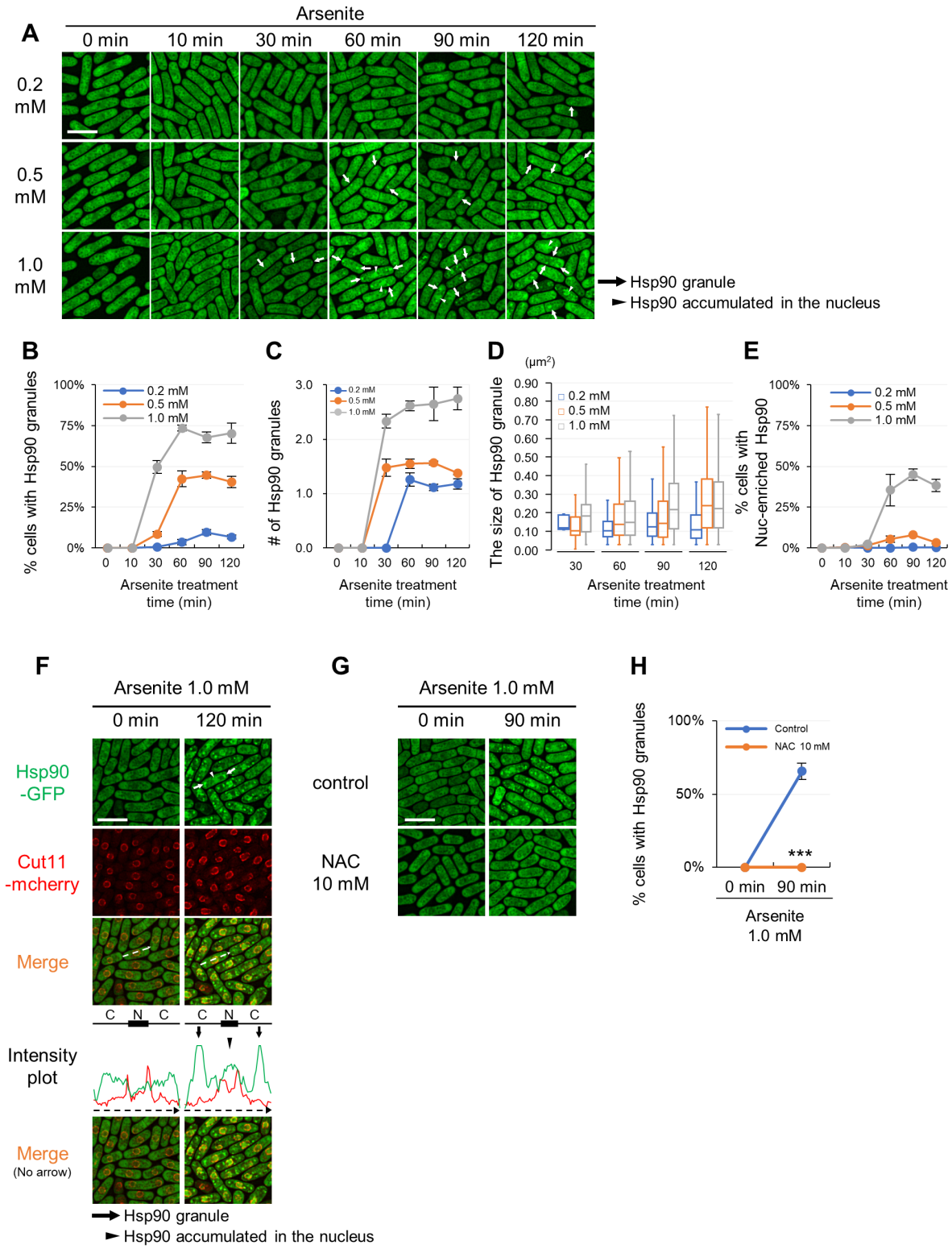

FIGURE 1 ● Hsp90 aggregates in the cytoplasm and accumulates in the nucleus upon arsenite stress via a ROS-involving mechanism. (A) Representative fluorescence images of the cells expressing GFP-tagged Hsp90 from its endogenous promoter under arsenite conditions (0.2 mM, 0.5 mM, and 1.0 mM) at 27°C. The minutes after arsenite addition are indicated above the images. (B) Percentage of the cells with Hsp90 granules. (C) The number of Hsp90 granules per cell in Hsp90 granule-positive cells. (D) The size of Hsp90 granules. The box signifies the 25-75th percentiles and the median is represented by a short line within the box. The whiskers show the range of data. (E) Percentage of the cells with Hsp90-enriched nucleus. (F) Line intensity plot of Hsp90-GFP (green) and Cut11-mcherry (red) for the representative image of the cells incubated with or without 1.0 mM arsenite for 120 min at 27°C. The dashed arrows in the merged images correspond to those below the intensity plot, and the line and box above the intensity plot indicate the positions of cytoplasm (C) and nucleus (N), respectively. (G) Effect of a ROS scavenger, n-acetylcysteine (NAC), on the arsenite-mediated Hsp90 granule formation. Cells were pre-incubated with or without 10 mM NAC for 2 min and then observed before or after treatment with 1.0 mM arsenite for 90 min at 27°C. (H) Percentage of Hsp90 granule-positive cells from (G). Scale bars: 10 μm. Arrows and arrowheads indicate representative Hsp90 granules and the Hsp90-enriched nuclei, respectively. The graphs show mean ± SE (n=3). P***<0.001; significantly different from each sample by paired Student's t-test.

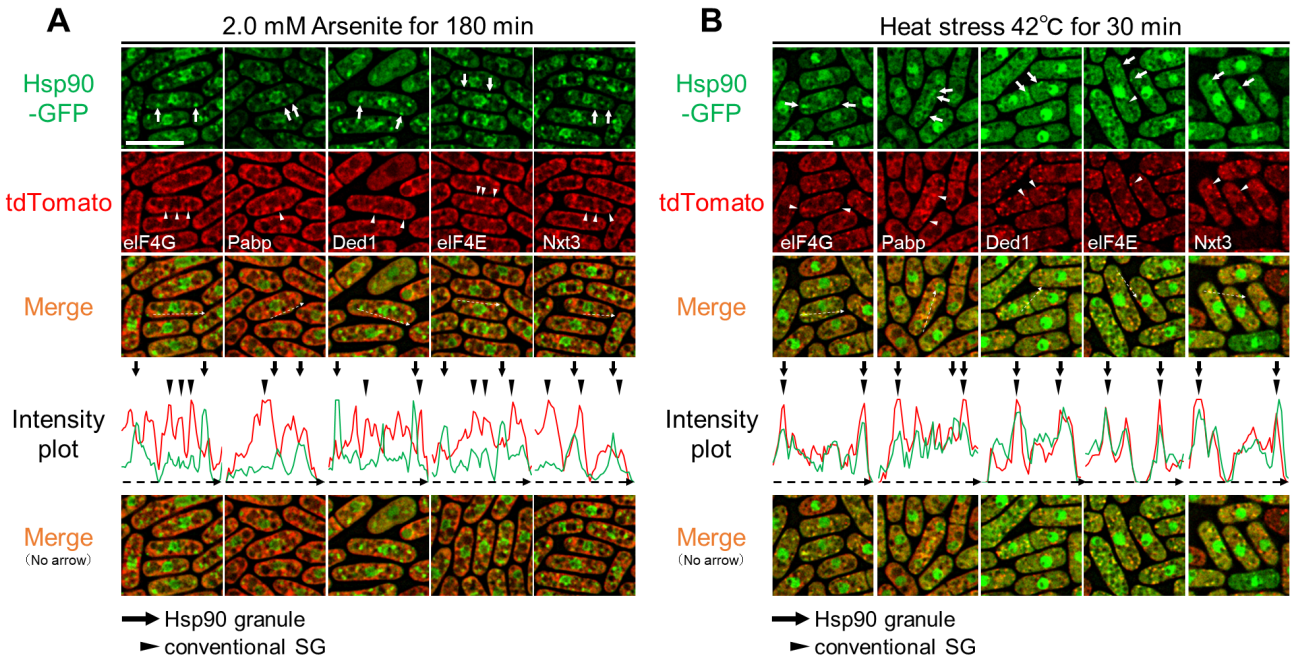

FIGURE 2 ● **Hsp90 granules co-localize with conventional SGs upon heat stress but not upon arsenite stress.** Co-localization analysis of Hsp90-GFP (green) and various SG markers tagged with tdTomato (red) after 2.0 mM arsenite treatment for 180 min at 27°C (**A**) or 42°C HS for 30 min (**B**). Arrows and arrowheads indicate representative Hsp90 granules and conventional SGs, respectively. The dashed arrows in the merged images correspond to those below the intensity plot. Scale bars: 10 μm. Co-localization of eIF4G and Pabp is shown in Fig. S3.

Hsp90 form cytoplasmic dot-like structures upon HS (42°C) for 30 min. Importantly, unlike arsenite treatment, HS induced co-localization of Hsp90 and the representative components of conventional SGs as evidenced by the fluorescence microscopy and its analysis by the intensity plot (**Figure 2B**). Thus, Hsp90 is a component of canonical SGs induced by HS but not that of arsenite-induced SGs.

As mentioned earlier, the formation of Hsp90 granules upon arsenite treatment depends on the intensity of the stress. We then tested whether increased concentrations or incubation times of arsenite treatment alter the behavior of Hsp90 granules and their relationship with SGs as visualized by Pabp. As a first step, we examined the conditions wherein the arsenite-mediated SGs are formed by varying incubation times and compound concentrations. The results showed that Pabp dots were observed 60 min after 2.0 mM or 5.0 mM arsenite treatment (Figure S4A). The Pabp granules persisted during 360 min incubation under both concentrations of arsenite. Next, we incubated the cells expressing Hsp90-GFP and Pabp-tdTomato with either 2.0 mM or 5.0 mM arsenite for up to 360 min. The results showed that 2.0 mM arsenite treatment for a longer incubation time (360 min) did not induce co-localization of Hsp90 and Pabp granules as evaluated by the intensity plot (Figure S4B). Furthermore, 5.0 mM arsenite treatment for 60 min did not induce co-localization of Pabp and Hsp90 granules. Notably, however, when cells were treated with 5.0 mM arsenite for 360 min, some cells showed co-localization of Hsp90 and Pabp granules (Figure S4B #2), although a large number of the cells exhibited Hsp90 granules and Pabp granules that do not merge (Figure S4B #1). Thus, even increased concentrations or incubation times of arsenite treatment rarely induce co-localization of Hsp90 and Pabp.

Nrd1 is a component of arsenite-mediated Hsp90-positive granules

We further investigated the co-localization of Hsp90 and an RNA-binding protein Nrd1, which we have previously shown to localize at SGs upon HS [19]. Nrd1-tdTomato was visualized in cells expressing Hsp90-GFP. The fluorescence of Nrd1 dots largely merged with that of Hsp90 granules upon HS and arsenite treatment, thus indicating that Nrd1 is a component of Hsp90-positive granules (**Figure 3A**, S5). We investigated whether Nrd1 co-localizes with components of conventional SGs under HS and arsenite treatment. The fluorescence of Nrd1-tdTomato dots induced by HS was co-localized with that of canonical SGs as visualized by eIF4G-GFP. In contrast, Nrd1 dots induced by arsenite did not overlap with canonical SGs (**Figure 3B**, S5). Thus, although both Hsp90 and Nrd1 localize at SGs upon HS, these proteins form aggregates different from conventional SGs induced by arsenite treatment.

To understand the relationship between Nrd1 and Hsp90 in arsenite-specific aggregate formation, a time-course analysis of intracellular localization of Hsp90 and Nrd1 was performed. As shown in **Figure 3C**, Hsp90 granules were observed within 30 min exposure to 2.0 mM arsenite, which persisted for 180 min. The Nrd1 dots were not observed upon 30 min incubation and appeared after 60 min arsenite treatment. Quantification of the number of cytoplasmic dots of each protein showed that Hsp90 granules showed a steep increase (up to 4-fold) within 30 min and lasted for 180 min incubation (**Figure 3D**). The number of Nrd1 dots per cell at 60 min incubation was much smaller than that of Hsp90 dots. However, during arsenite treatment for

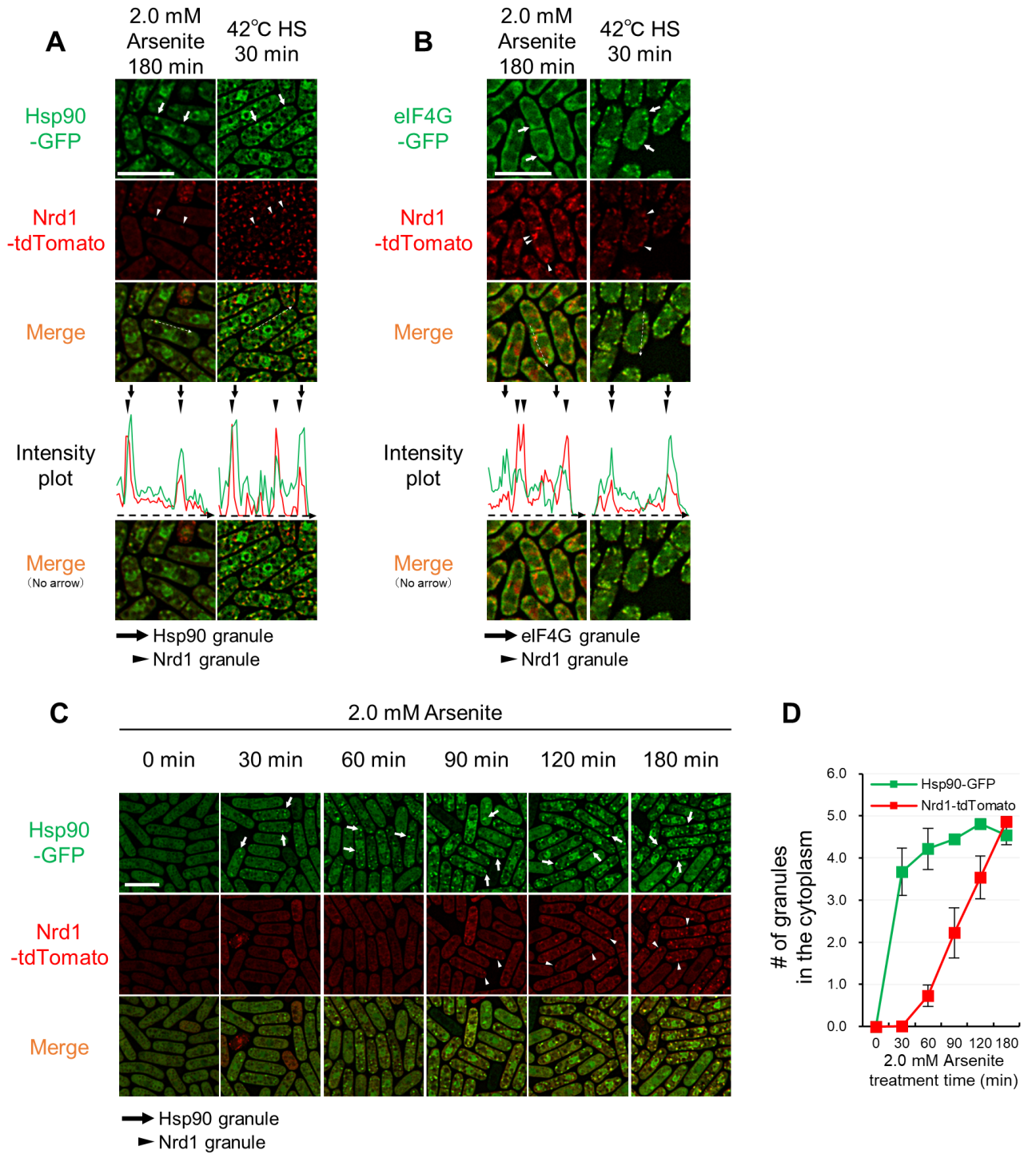

FIGURE 3 ● **Nrd1 co-localizes with Hsp90 granules, but not with SGs, upon arsenite stress.** (A, B) Co-localization analysis of Nrd1-tdTomato (red) and Hsp90-GFP (green) (A) or eIF4G-GFP (green) (B) after 2.0 mM arsenite treatment for 180 min at 27°C (A) or 42°C HS for 30 min. Arrows indicate representative Hsp90 granules or eIF4G granules, and arrowheads indicate representative Nrd1 granules. The dashed arrows in the merged images correspond to those below the intensity plot. (C) Nrd1 granule formation is slower than that of Hsp90. Representative images of the cells expressing Hsp90-GFP (green) and Nrd1-tdTomato (red) from their own promoters upon 2.0 mM arsenite treatment for the indicated times at 27°C. Arrows and arrowheads indicate representative Hsp90 granules and Nrd1 granules, respectively. Scale bars: 10 μm. (D) The number of Hsp90 granules (green) and Nrd1 granules (red) per cell from (C). The graphs show mean ± SE (n=3).

180 min, Nrd1 dots gradually increased and reached a number similar to that of Hsp90 dots per cell (Figure 3D).

Severe arsenite treatment induces irreversible Hsp90/Nrd1 aggregates

Next, we tested if arsenite-induced Hsp90/Nrd1 granules are reversible upon arsenite removal by following their behavior with fluorescence microscopy (Figure 4). First, 1.0 mM arsenite treatment for 90 min induced reversible granules as evidenced by the significantly reduced number of cells with Hsp90 granules (reduced from 75% to 10%) evaluated 240 min after the arsenite removal from the medium. In contrast, 2.0 mM arsenite treatment for 90 min induced less reversible Hsp90 granules than did 1.0 mM arsenite treatment, since the percentages of cells with Hsp90 granules were reduced by only 20 percentage points, from 85% to 65%, even 4 h after removing arsenite from the medium. 2.0 mM arsenite treatment for 180 min induced more irreversible Hsp90 granules than did 90 min treatment. Upon 1.0 mM arsenite treatment for 90 min, only a limited number of cells showed Nrd1 granules, which was almost abolished after removing arsenite for 4 h. 2.0 mM arsenite treatment for 90 min induced Nrd1 granules in 65% of cells and the percentages were dropped to 25% after 4 h removal, Notably, 2.0 mM arsenite treatment for 180 min induced Nrd1 granules in most of the cells and the granules were irreversible even after 4 h removal of arsenite from the medium. Furthermore, 2.0 mM arsenite treatment for 180 min induced the most irreversible granules in terms of the persistence of the aggregation of both Hsp90 and Nrd1 even after 4 h arsenite removal from the medium. These data suggest that the longer and more intense arsenite treatment induces the more difficult-to-disperse Hsp90/Nrd1 granules. We also tested cell viability after arsenite treatment, and the results showed that cells treated with each condition of arsenite treatment did not show defects in cell viability compared with cells treated with the vehicle (Figure S6). Thus, the irreversible Hsp90 aggregation may not be derived from cell death.

The impact of non-phosphorylatable eIF2α mutation and cycloheximide on Hsp90/Nrd1 granule formation

In mammalian cells, phosphorylation of the translation initiation factor eIF2α plays a key role in SG formation, and the expression of a non-phosphorylatable version of eIF2α was shown to block SG formation [1]. In fission yeast, Sunnerhagen's lab investigated the effect of the corresponding fission yeast non-phosphorylatable eIF2α-S52A mutant and showed that the eIF2α-S52A mutation slowed the appearance of SGs (as visualized by Pabp) upon KCl stress [21]. As a first step to know whether the same mechanism also regulates arsenite-mediated Hsp90 granules formation, we investigated the effect of the eIF2α-S52A mutation on the arsenite-mediated Hsp90/Nrd1 granules. For this, we co-expressed Hsp90-GFP and Nrd1-tdTomato in a strain expressing the eIF2α-S52A mutant protein. As shown in Figures 5A and B, the number of Hsp90 granules 30 min after the 2.0 mM arsenite treatment in the eIF2α-S52A mutant cells was significantly lower as compared with that of the wild-type (WT) cells. After 60 min arsenite treatment, the number of Hsp90 granules in the eIF2α-S52A mutants and WT cells were indistinguishable, suggesting that the eIF2α-S52A mutation delayed the formation of Hsp90 granules upon arsenite treatment. In contrast, the number and the kinetics of Nrd1 granules upon arsenite treatment were not significantly affected by the eIF2α-S52A mutation (Figure 5A and B).

As a second step, we examined the effect of cycloheximide (CHX), which freezes ribosomes in place by inhibiting translation elongation, on the induction of the Hsp90 aggregation. Cells expressing Hsp90-GFP were simultaneously treated with CHX and arsenite, and the results showed that CHX significantly impaired the arsenite-induced aggregation of Hsp90 (Figure 5C). Similarly, the co-treatment with CHX significantly diminished Nrd1 granules upon arsenite treatment (Figure 5C). Quantification of the number of Hsp90 and Nrd1 granules also confirmed the observations (Figure 5D). Thus, the aggregation of Hsp90 and Nrd1 requires a free mRNA, a translation event, or a newly translated protein for their formation. We also examined the expression levels of Hsp90 and Nrd1 upon arsenite treatment using immunoblotting to complement the immunofluorescence data and confirmed that CHX did not affect the protein levels of Hsp90 and Nrd1, indicating that the effect of CHX can be attributed to condensation and not overall Hsp90 or Nrd1 levels (Figure S7).

The role of Hsp90 in the formation of Hsp90/Nrd1 granules

Next, we investigated the effect of Hsp90 inhibition on Nrd1 recruitment into Hsp90 granules using an Hsp90 inhibitor geldanamycin (GA). For this, cells expressing Hsp90-GFP and Nrd1-tdTomato from their endogenous promoters were pre-treated with 10 μM GA for 20 h, followed by treatment with 2.0 mM arsenite for 150 min. The results showed that GA treatment significantly reduced the formation of arsenite-induced Hsp90/Nrd1 granules (Figure 6A). Quantification of the percentages of the cells harboring Hsp90 granules or Nrd1 granules showed that both decreased by approximately 50% (Figure 6B). Thus, Hsp90 inhibition by GA reduced the formation of Hsp90 granule assembly and recruitment of Nrd1 to Hsp90 granules, consistent with the hypothesis that Hsp90 might function as a seeding element recruiting other components as represented by Nrd1.

Regarding cell viability upon GA treatment, 10.0 μM GA did not significantly affect the cell viability of the WT cells (Figure S8A). It should be noted that the cell length became significantly smaller when treated with GA for 20 h (Figure S8B, S8C). Notably, however, the growth of the WT cells was significantly impaired when co-treated with GA and arsenite. For example, 0.5 mM arsenite did not significantly affect cell growth, whereas the simultaneous adding 10.0 μM GA almost abolished cell growth (Figure 6C). From these results, we hypothesize that the induction of arsenite-mediated Hsp90 granule formation is beneficial for cell survival under arsenite stress, and the inhibition of Hsp90 by GA may hamper cell growth by impairing the cell survival mechanism.

DISCUSSION

SG is a conservative mechanism that cells have developed to adapt to various stresses and the list of SG-promoting stimuli continues to grow [22]. SGs have been generally assumed to be uniform despite different stressors. However, some evidence shows that their composition varies according to the stress,

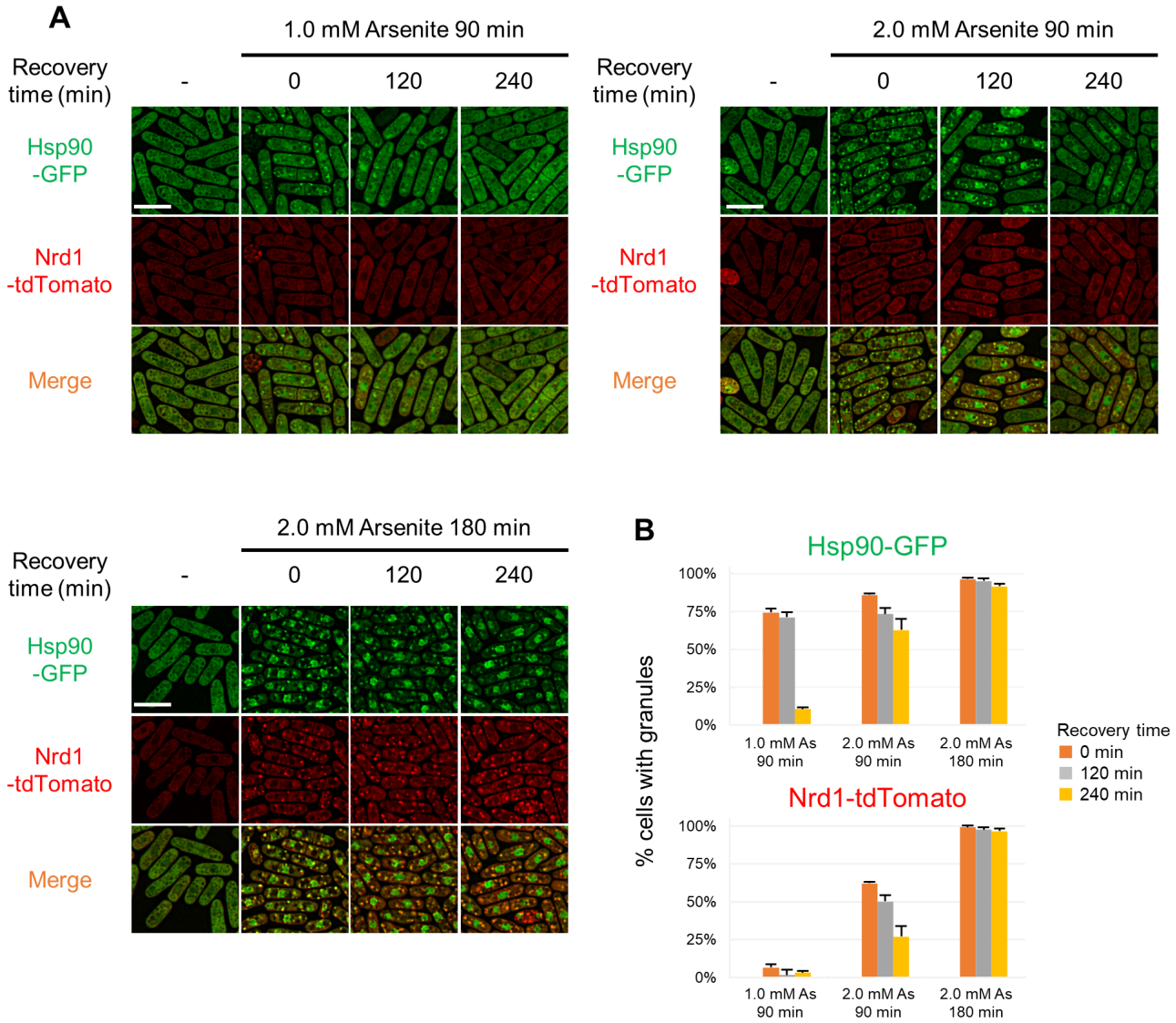

FIGURE 4 ● **Reversibility of Hsp90/Nrd1 granules upon arsenite removal.** (**A**) Representative fluorescence images of Hsp90/Nrd1 granules in the cells released from arsenite stress. Cells expressing Hsp90-GFP (green) and Nrd1-tdTomato (red) were treated with 1.0 mM or 2.0 mM arsenite for 90 min or 2.0 mM Arsenite for 180 min at 27°C and then recovered in the fresh medium without arsenite for 120 min or 240 min at 27 °C. (**B**) Percentage of the cells with Hsp90 granules or Nrd1 granules. The graphs show mean ± SE (n=3).

suggesting the existence of stress-specific SG subtypes [1]. Therefore, SGs can assemble differently at least in terms of components in response to specific cellular stresses [23]. However, no clear evidence has been reported as to whether a regulatory mechanism that differentially compartmentalizes specific cellular components into different biomolecular condensates may exist.

Here, we have characterized the stress-specific spatiotemporal distribution of Hsp90 and provided evidence that HS and arsenite differentially compartmentalize Hsp90 in and out of the SGs, respectively. Firstly, arsenite treatment induced cytoplasmic Hsp90 aggregates in a dose-dependent manner (**Figure 1**). Secondly, we have demonstrated that Hsp90 resides in conventional SGs upon HS but not upon arsenite by visualizing the co-localization of Hsp90 and each component of SGs (**Figure 2**). The absence of the Hsp90 co-localization with representative components of conventional SGs demonstrated that Hsp90 forms aggregates distinct from conventional SGs upon arsenite treatment. Thirdly, HS, but not arsenite, targets Hsp90 and an RNA-binding protein Nrd1 in conventional SGs (**Figure 3**), suggesting the existence of a stress-specific mechanism that compartmentalizes selective molecules. Finally, inhibition of Hsp90 by geldanamycin impaired the Hsp90/Nrd1 aggregates and reduced the arsenite tolerance (**Figure 6**), suggesting that Hsp90 plays a key role as a center for aggregation of this novel type of biological condensates.

Thus far, the fate of each client protein to be sequestered into SGs has been considered to be triggered by each stimulus above a certain threshold. For example, severe HS (at 42°C) but not modest HS (at 37°C) can induce conventional SGs [18]. These results suggest that environmental stresses above

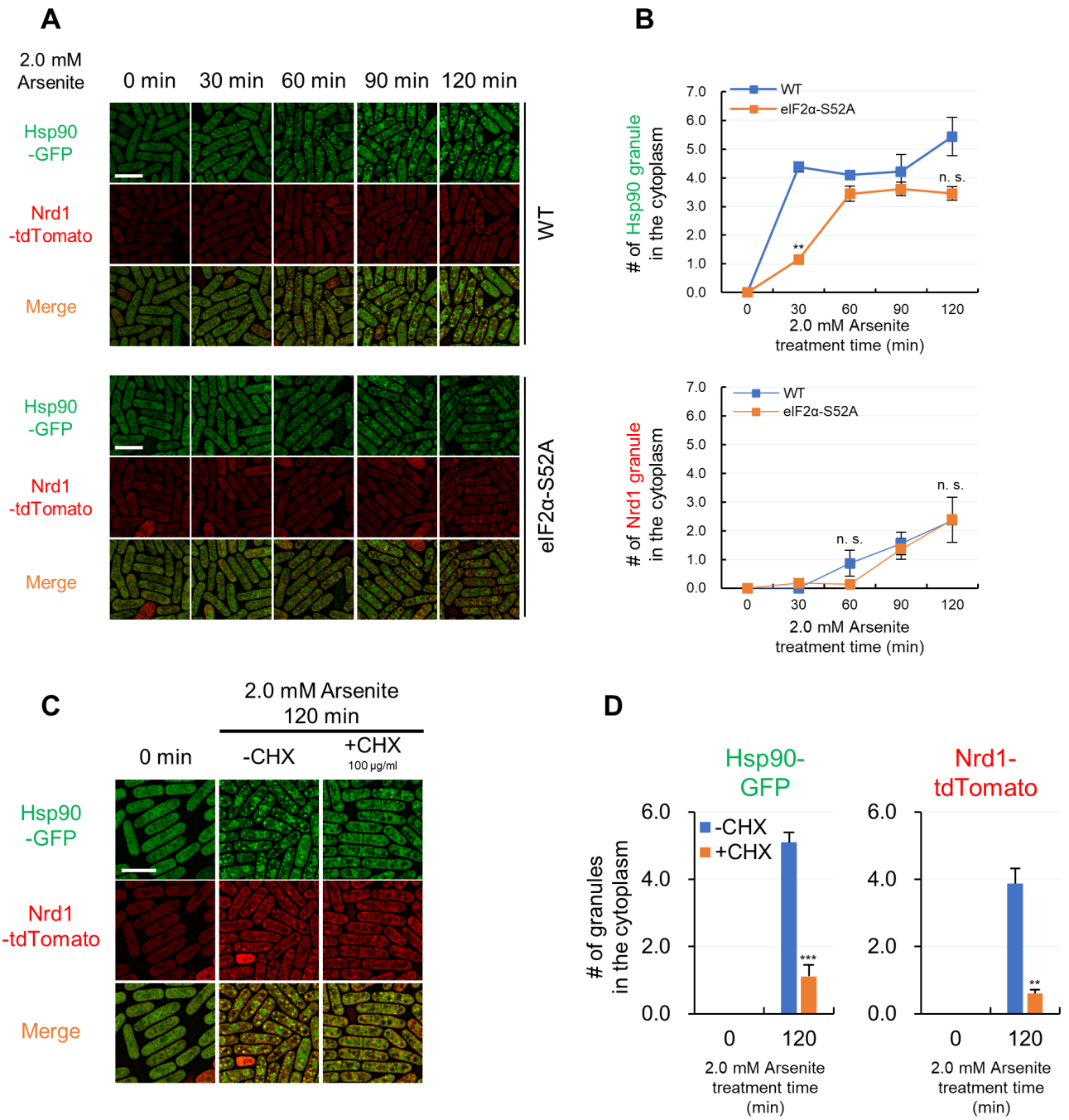

FIGURE 5 ● **Hsp90/Nrd1 granule formation is delayed by non-phosphorylatable eIF2α mutation and inhibited by cycloheximide.** (**A**) Representative fluorescence images of Hsp90-GFP and Nrd1-tdTomato in the wild-type cells (WT) and non-phosphorylatable eIF2α-S52A mutant cells (eIF2α-S52A) upon 2.0 mM arsenite treatment for the indicated times at 27°C. (**B**) The number of Hsp90 granules and Nrd1 granules in WT cells (blue) and eIF2α-S52A cells (orange) per cell. (**C**) Effect of cycloheximide (CHX) on the arsenite-mediated Hsp90/Nrd1 granule formation. Cells were pre-incubated with or without 100 μg/ml CHX for 10 min and then observed after 2.0 mM arsenite treatment for 120 min at 27°C. (**D**) The number of Hsp90 granules and Nrd1 granules per cell. The graphs show mean ± SE (n=3). P**<**0.05, P**<**0.01, P**<**0.001; n. s., not significant; significantly different from each sample by paired Student's t-test. Scale bars: 10 μm.

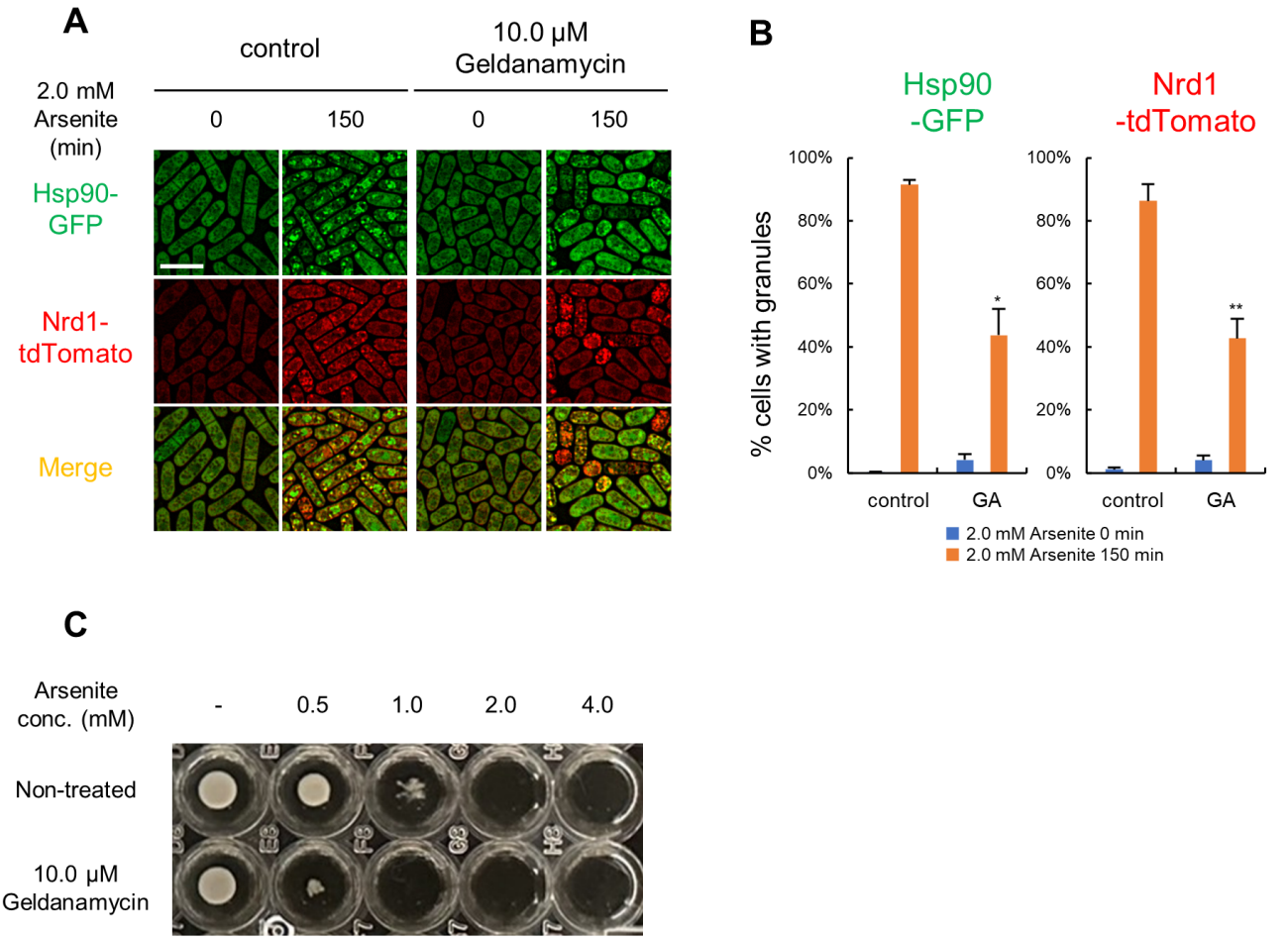

FIGURE 6 ● **Geldanamycin decreases Hsp90/Nrd1 granules and increases the arsenite sensitivity.** (**A**) Cells expressing Hsp90-GFP (green) and Nrd1-tdTomato (red) were pre-incubated with or without 10.0 μM GA for 20 hr and then treated with 2.0 mM arsenite for 150 min at 27°C. Scale bar: 10 μm. (**B**) Percentage of Hsp90 or Nrd1 granule positive cells. The graphs show mean ± SE (n=3). GA; geldanamycin. P∗<0.05, P∗∗<0.01; n. s., not significant; significantly different from each sample by paired Student's t-test. (**C**) Effect of GA on the arsenite sensitivity. Cells were grown in the EMM to mid-log phase with 0.56% DMSO or 10.0 μM GA and adjusted to OD660 = 0.5. The cells were then diluted 300-fold with the fresh EMM containing DMSO or 10.0 μM GA and incubated in a 96-well plate with the indicated final concentrations of arsenite for 4 days at 27°C.

some critical intensities facilitate client protein crowding (through physical interaction or post-translational modification), thus sequestration into SGs. However, our current findings suggested the presence of an additional layer of the stress-dependent regulatory mechanism of macromolecular crowding, which dictates the fate of a specific set of client proteins to be differentially compartmentalized into selective biological condensates, including SGs. As Hsp90 is well-known as a kinase-chaperone with special responsibility for the folding of protein kinases, HS and arsenite may stimulate distinct kinase signaling, which leads to different translational modifications of Hsp90/client protein and their coalescence in and out of the conventional SGs.

Relationships between conventional SGs and a novel type of Hsp90 granules

Although Hsp90 is known to play a key role in the assembly of biomolecular condensates such as P-bodies and SGs, the information on the stress-induced Hsp90 aggregation has been poorly understood. A recent paper by Hidalgo's group has reported that upon mild HS wherein SGs do not assemble, misfolded proteins collapse into protein aggregate centers (PACs), and many Hsp proteins, including Hsp90, are recruited into PACs [24]. PACs function to protect thermosensitive proteins contained in the PACs from degradation, which helps cells survive environmental insults [24]. Interestingly, the PACs formed upon mild HS transform into SGs by increasing the temperature or time of HS treatment, thus suggesting that PACs seem to be a seed for SGs formation upon more challenging conditions.

This study prompted us to investigate whether the arsenite-mediated Hsp90 granules may serve as a seed for SG formation by following the behavior of Hsp90 and Pabp under more intense arsenite treatment conditions. However, even extremely challenging arsenite treatment induced only a partial overlap of Hsp90 and Pabp (Figure S4B), thus suggesting that arsenite-induced Hsp90 granules and SGs seem distinct biomolecular condensates. However, since distinct biomolecular condensates, represented by SGs and P-bodies, often interchange their components, future proteomic

studies will elucidate the shared or distinct components of Hsp90 granules and conventional SGs.

Regulatory mechanisms of novel Hsp90 granules upon arsenite treatment

We have shown that Hsp90 granules and conventional SGs share some common regulatory mechanisms. Firstly, arsenite is the most commonly used agent to induce oxidative stress, which leads to stalled translation initiation and the formation of SGs [2]. It has been reported that arsenite-induced SG formation is inhibited by elevated levels of reduced glutathione, an antioxidant that neutralizes ROS, in West Nile virus-infected cells [25]. We also showed that Hsp90-positive granule formation was impaired by NAC, indicating that ROS is responsible for Hsp90-positive granule assembly (Figure 1G, 1H). SGs generally assemble in response to stresses through stress-induced inhibition of translation initiation [8]. Thus, both Hsp90 granules and conventional SGs coincide with translation inhibition mediated by oxidative stress induced by arsenite treatment.

Secondly, non-phosphorylatable eIF2α mutation significantly delayed the arsenite-induced aggregation of Hsp90 (Figure 5A, 5B), similar to the slow appearance of SGs observed in eIF2α-S52A mutant [21]. Thus, SGs and Hsp90-positive granules appear to require similar regulatory mechanisms to induce their formation, at least in part. We also showed that CHX, a well-known inhibitor of SG formation, significantly impaired the arsenite-induced Hsp90 aggregation (Figure 5C, 5D). CHX is a protein synthesis inhibitor that blocks the progression of 80s ribosomes along mRNA and stabilizes polysomes, therefore reducing polysome-free mRNAs as well as newly translated proteins. To clarify the crucial processes for Hsp90 granule formation upon arsenite treatment, we tried to inhibit translation through other ways than blocking the release of polysome from mRNAs. Translation can be impaired due to decreased translation initiation rates [1], stalling initiation [9], or blocking elongation [10]. However, other translation inhibitors, neither harringtonine nor puromycin effectively inhibit translation in our culture conditions and we could not confirm the effects of these drugs on arsenite-mediated Hsp90 granules. We, therefore, assume that our CHX experiment has limitations.

Role of the nuclear translocation of Hsp90 upon arsenite treatment

Regarding the nuclear translocation of Hsp90 upon arsenite treatment, a similar stress-induced Hsp90 nuclear enrichment was observed with HS, which also induces cytoplasmic Hsp90 aggregates. Despite its primary role as a cytoplasmic protein, Hsp90 also impacts various functions in the nucleus, including transcription, chromatin remodeling, and DNA damage-induced mutation [26]. Thus, arsenite-mediated nuclear translocation of Hsp90 and its functional significance will be the issue of future study.

Role of Hsp90 in novel arsenite-mediated granules

Recently, the property of molecular chaperones, such as Hsp70, to serve as a nucleation center for biological condensates has attracted strong attention [24]. We have shown several data suggesting that Hsp90 aggregates may serve as an arsenite-specific protein aggregation center. First, even the low concentration of 0.2 mM arsenite induces Hsp90 aggregation (Figure 1). Second, an RNA-binding protein Nrd1 is sequestered into Hsp90-positive granules upon arsenite treatment suggesting the possible role of Hsp90 in recruiting Nrd1 in Hsp90-positive granules (Figure 3). Finally. inhibition of Hsp90 by geldanamycin repressed the formation of Hsp90/Nrd1 granules further supporting the role of Hsp90 as an aggregation center (Figure 6A, 6B). Why and how Hsp90 and Nrd1 form aggregates outside conventional SGs remains unknown. However, the finding that Hsp90 inhibition by GA reduced the cells' tolerance to arsenite (Figure 6C), suggested the role of Hsp90 for survival under arsenite stress. However, we cannot rule out the possibility that the combination of GA and arsenite may induce a synthetic lethal effect regardless of the formation of Hsp90/Nrd1 granules. Future intensive studies may reveal the stress-specific condensates' composition and biological properties.

In summary, this is the first demonstration that arsenite stimuli can differentially compartmentalize two biological condensates with or without Hsp90. Given the conserved role of Hsp90 and SGs, our findings may shed light on the underlying mechanisms of various diseases associated with SGs.

MATERIALS AND METHODS

Yeast strain, media, and molecular biology

Schizosaccharomyces pombe strains and plasmids used in this study are listed in Table S1. The completed medium (Yeast Extract with Supplements [YES]) and the minimal medium (Edinburgh Minimal Medium [EMM]) have been described previously [27]. Except where noted, standard yeast culture and genetic methods were used [27]. GFP and tdTomato were tagged on the C-terminal side of the respective genes using the PCR-based genomic tagging method [28].

Growth conditions and stress treatment

Before stress treatment, the cells harboring plasmid that contains the LEU2 gene were grown to mid-log phase at 27°C in EMM. After cultivation, Reagents (listed in Table S2) at the indicated concentrations were added to the culture medium, or cells were heat-shocked at 42°C in the water bath for the stated time. After each stress treatment, the culture medium was chilled in ice water for a minute. The cells were harvested by brief centrifugation at 4°C.

Microscopy and image quantitation

Images were captured by All-in-One Fluorescence Microscope BZ-X710 equipped with an optical sectioning module (Keyence, Osaka, Japan). Image processing for haze reduction and granule quantitation was done with BZ-X Analyzer software (Keyence, Osaka, Japan). We performed three independent experiments, imaging more than 100 cells in each experiment and analyzing the granule counts and nuclear translocation.

Protein extraction (alkaline extraction) and detection

Cell extract preparation was performed as previously described [29]. The following primary antibodies were used: anti-GFP (sc-9996, Santa Cruz Biotechnology, USA), anti-RFP (PM005, Medical, and Biological Laboratories, Japan), and

anti-α-tubulin (T5168, Sigma-Aldrich, St. Louis, MO, USA.) As a secondary antibody, anti-rabbit IgG HRP-linked antibody (#7074, Cell signaling Technology, USA) or Goat anti-mouse IgG (H+L) Alexa Fluor™ Plus 555 highly cross-adsored (#A32727: Thermo Fisher Scientific, USA) were used. The proteins were detected by Chemi-Lumi One L (Nacalai Tesque, Japan) or excitation light with Amersham™ ImageQuant™ 800 (Cytiva, Japan). The imaging was performed using Amersham™ ImageQuant™ 800 (Cytiva, Japan), and the protein bands were quantified using ImageQuant™ TL (Cytiva, Japan).

Statistical analysis

All results are expressed as means ± Standard Error of the mean (SE) of three independent experiments. Data were analyzed using Student's t-test. Statistical significance was defined as $p*<0.05$, $p**<0.01$, $p***<0.001$, n. s.; not significant.

ACKNOWLEDGMENTS

We thank Dr. Mitsuhiro Yanagida for providing the mCherry-tagged Cut11 strain, and the members of Sugiura Lab for discussion and technical support. This study was supported by JSPS KAKENHI Grant Numbers JP20K07058 and JP24K09826 (Teruaki Takasaki) and JP19H03376 (Reiko Sugiura). This work was also supported by a grant from the Antiaging Project for Private Universities (Reiko Sugiura).

SUPPLEMENTAL MATERIAL

All supplemental data for this article are available online at www.microbialcell.com.

CONFLICT OF INTEREST

The authors declare that the research was conducted in the absence of any commercial or financial relationships that could be construed as a potential conflict of interest.

COPYRIGHT

Please cite this article as: Naofumi Tomimoto, Teruaki Takasaki, Reiko Sugiura (2024). Arsenite treatment induces Hsp90 aggregates distinct from conventional stress granules in fission yeast. Microbial Cell 11: 242-253. doi: 10.15698/mic2024.07.829

References

1. Kedersha NL, Gupta M, Li W, Miller I, Anderson P (1999). RNA-binding proteins TIA-1 and TIAR link the phosphorylation of eIF-2 alpha to the assembly of mammalian stress granules. J Cell Biol 147 (7): 1431–1442. doi: 10.1083/jcb.147.7.1431

2. Kedersha N, Stoecklin G, Ayodele M, Yacono P, Lykke-Andersen J, Fritzler MJ, Scheuner D, Kaufman RJ, Golan DE, Anderson P (2005). Stress granules and processing bodies are dynamically linked sites of mRNP remodeling. J Cell Biol 169 (6): 871–884. doi:10.1083/jcb.200502088

3. Moeller BJ, Cao Y, Li CY, Dewhirst MW (2004). Radiation activates HIF-1 to regulate vascular radiosensitivity in tumors: role of reoxygenation, free radicals, and stress granules. Cancer Cell 5 (5): 429–441. doi:10.1016/s1535-6108(04)00115-1

4. Aulas A, Lyons SM, Fay MM, Anderson P, Ivanov P (2018). Nitric oxide triggers the assembly of "type II" stress granules linked to decreased cell viability. Cell Death Dis 9 (11): 1129–1129. doi:10.1038/s41419-018-1173-x

5. Emara MM, Fujimura K, Sciaranghella D, Ivanova V, Ivanov P, Anderson P (2012). Hydrogen peroxide induces stress granule formation independent of eIF2alpha phosphorylation. Biochem Biophys Res Commun 423 (4): 763–769. doi:10.1016/j.bbrc.2012.06.033

6. Kedersha N, Chen S, Gilks N, Li W, Miller IJ, Stahl J, Anderson P (2002). Evidence that ternary complex (eIF2-GTP-tRNA(i)(Met))-deficient preinitiation complexes are core constituents of mammalian stress granules. Mol Biol Cell 13 (1): 195–210. doi:10.1091/mbc.01-05-0221

7. Reineke LC, Cheema SA, Dubrulle J, Neilson JR (2018). Chronic starvation induces noncanonical pro-death stress granules. J Cell Sci 131: 220,244–220,244. doi:10.1242/jcs.220244

8. Kedersha N, Anderson P (2002). Stress granules: sites of mRNA triage that regulate mRNA stability and translatability. Biochem Soc Trans 30: 963–969. doi:10.1042/bst0300963

9. Arimoto K, Fukuda H, Imajoh-Ohmi S, Saito H, Takekawa M (2008). Formation of stress granules inhibits apoptosis by suppressing stress-responsive MAPK pathways. Nature Cell Biology 10 (11): 1324–1332. doi: 10.1038/ncb1791

10. Thedieck K, Holzwarth B, Prentzell MT, Boehlke C, Klasener K, Ruf S, Sonntag AG, Maerz L, Grellscheid SN, Kremmer E, Nitschke R, Kuehn EW, Jonker JW, Groen AK, Reth M, Hall MN, Baumeister R (2013). Inhibition of mTORC1 by astrin and stress granules prevents apoptosis in cancer cells. Cell 154 (4): 859–874. doi:10.1016/j.cell.2013.07.031

11. Wippich F, Bodenmiller B, Trajkovska MG, Wanka S, Aebersold R, Pelkmans L (2013). Dual specificity kinase DYRK3 couples stress granule condensation/dissolution to mTORC1 signaling. Cell 152 (4): 791–805. doi: 10.1016/j.cell.2013.01.033

12. Kanda Y, Satoh R, Takasaki T, Tomimoto N, Tsuchiya K, Tsai CA, Tanaka T, Kyomoto S, Hamada K, Fujiwara T, Sugiura R (2021). Sequestration of the PKC ortholog Pck2 in stress granules as a feedback mechanism of MAPK signaling in fission yeast. J Cell Sci 134 (2): 250,191–250,191. doi:10.1242/jcs.250191

13. Markmiller S, Soltanieh S, Server KL, Mak R, Jin W, Fang MY, Luo EC, Krach F, Yang D, Sen A, Fulzele A, Wozniak JM, Gonzalez DJ, Kankel MW, Gao FB, Bennett EJ, Lecuyer E, Yeo GW (2018). Context-Dependent and Disease-Specific Diversity in Protein Interactions within Stress Granules. Cell 172 (3): 590–604. doi:10.1016/j.cell.2017.12.032

14. Youn JY, Dunham WH, Hong SJ, Knight J, Bashkurov M, Chen GI, Bagci H, Rathod B, Macleod G, Eng S, Angers S, Morris Q, Fabian M, Cote JF, Gingras AC (2018). High-Density Proximity Mapping Reveals the Subcellular Organization of mRNA-Associated Granules and Bodies. Mol Cell 69 (3): 517–532. doi: 10.1016/j.molcel.2017.12.020

15. Young JC, Moarefi I, Hartl FU (2001). Hsp90: a specialized but essential protein-folding tool. J Cell Biol 154 (2): 267–273. doi:10.1083/jcb.200104079

16. Richter K, Buchner J (2001). Hsp90: chaperoning signal transduction. J Cell Physiol 188 (3): 281–290. doi:10.1002/jcp.1131

17. Richter K, Haslbeck M, Buchner J (2010). The heat shock response: life on the verge of death. Mol Cell 40 (2): 253–266. doi:10.1016/j.molcel.2010.10.006

18. Takasaki T, Tomimoto N, Ikehata T, Satoh R, Sugiura R (2021). Distinct spatiotemporal distribution of Hsp90 under high-heat and mild-heat stress conditions in fission yeast. MicroPubl Biol doi:10.17912/micropub.biology.000388

19. Satoh R, Tanaka A, Kita A, Morita T, Matsumura Y, Umeda N, Takada M, Hayashi S, Tani T, Shinmyozu K, Sugiura R (2012). Role of the RNA-binding protein Nrd1 in stress granule formation and its implication in the stress response in fission yeast. PLoS One 7 (1): 29,683–29,683. doi:10.1371/journal.pone.0029683

20. Wu L, Yi H, Zhang H (**2013**). Reactive oxygen species and Ca2+ are involved in sodium arsenite-induced cell killing in yeast cells. **FEMS Microbiol Lett** 343 (1): 57–63. doi:10.1111/1574-6968.12131

21. Nilsson D, Sunnerhagen P (**2011**). Cellular stress induces cytoplasmic RNA granules in fission yeast. **RNA** 17 (1): 120–133. doi:10.1261/rna.2268111

22. Aulas A, Vande Velde, C (**2015**). Alterations in stress granule dynamics driven by TDP-43 and FUS: a link to pathological inclusions in ALS? **Front Cell Neurosci** 9: 423–423. doi:10.3389/fncel.2015.00423

23. Protter DSW, Parker R (**2016**). Principles and Properties of Stress Granules. **Trends Cell Biol** 26 (9): 668–679. doi:10.1016/j.tcb.2016.05.004

24. Cabrera M, Boronat S, Marte L, Vega M, Perez P, Ayte J, Hidalgo E (**2020**). Chaperone-Facilitated Aggregation of Thermo-Sensitive Proteins Shields Them from Degradation during Heat Stress. **Cell Rep** 30 (7): 2430–2443. doi:10.1016/j.celrep.2020.01.077

25. Basu M, Courtney SC, Brinton MA (**2017**). Arsenite-induced stress granule formation is inhibited by elevated levels of reduced glutathione in West Nile virus-infected cells. **PLoS Pathog** 13 (2): 1006,240–1006,240. doi:10.1371/journal.ppat.1006240

26. Pennisi R, Ascenzi P, di Masi A (**2015**). Hsp90: A New Player in DNA Repair? **Biomolecules** 5 (4): 2589–2618. doi:10.3390/biom5042589

27. Sabatinos SA, Forsburg SL (**2010**). Molecular genetics of Schizosaccharomyces pombe. **Methods Enzymol** 470: 759–795. doi:10.1016/S0076-6879(10)70032-X

28. Bahler J, Wu JQ, Longtine MS, Shah NG, 3rd AM, Stever AB, Wach A, Philippsen P, Pringle JR (**1998**). Heterologous modules for efficient and versatile PCR-based gene targeting in Schizosaccharomyces pombe. **Yeast** 14 (10): 943–951. doi:10.1002/(SICI)1097-0061(199807)14:10<943::AID-YEA292>3.0.CO;2-Y

29. Kushnirov VV (**2000**). Rapid and reliable protein extraction from yeast. **Yeast** 16 (9): 857–860. doi:10.1002/1097-0061(20000630)16:9<857::AID-YEA561>3.0.CO;2-B

30. Hayashi T, Teruya T, Chaleckis R, Morigasaki S, Yanagida M (**2018**). S-Adenosylmethionine Synthetase Is Required for Cell Growth, Maintenance of G0 Phase, and Termination of Quiescence in Fission Yeast. **iScience** 5: 38–51. doi:10.1016/j.isci.2018.06.011